

Separation of Individual Thermal Double-Donor Levels by Laplace Deep-Level Transient Spectroscopy

Katarzyna Gwozdz, Vladimir Kolkovsky,* and Joerg Weber

Thermal double donors (TDDs) are created by heat treatment of Czochralski-grown Si at temperatures around 450 °C. A family of individual defects with very similar donor ($\text{TDDn}^{0/+}$ with $n = 0\text{--}16$) and double-donor ($\text{TDDn}^{+/++}$) levels is known today. The close-level positions of the individual TDDs result in broad and asymmetric deep-level transient spectroscopy (DLTS) peaks. Herein, Laplace DLTS are used to study this asymmetry. Several well-separated Laplace DLTS peaks are resolved in our samples. Metastable properties of the TDDs are taken as advantages to identify the double-donor levels ($+/+$) of TDD0, TDD1, and TDD2.

1. Introduction

Thermal double donors (TDDn) in silicon are known since the 1950s. They are successively created in Si samples with a high oxygen content (around 10^{18} cm^{-3}) during heat treatments at 350–550 °C.^[1–3] The recently renewed interest in oxygen-related TDDs is connected with the application of *n*-type Czochralski (CZ) Si in photovoltaics.^[4–6] To date, up to 17 different effective mass-like double-donor species (TDD0–TDD16) have been reported in the literature.^[7–9] In IR absorption, the effective mass-like transitions of the neutral charge state TDDn^0 and the singly ionized charge state TDDn^+ revealed the close spacing of the binding energies for the donor and double-donor states of individual TDDs. Longer heat treatments create TDDs with larger *n* and smaller binding energies. The binding energies for donor and double-donor states for all TDDn are found in the vicinity of 0.05 eV ($0/+$) and 0.15 eV ($+/++$) below the bottom of the conduction band, respectively.^[9] Deep-level transient

spectroscopy (DLTS) could not resolve the individual TDDs but detected two asymmetric peaks at the average energies of the donor and double-donor state.^[10]

The first species TDD0 to TDD2 are bistable defects with negative-U properties. These defects exist in two configurations with very different electronic properties: the stable configuration S is a deep donor with a large electron-binding energy, whereas the other metastable configuration M has the two electronic levels of a shallow double donor.^[11–16]

The occupation of the S- or M-configuration depends on the location of the Fermi level with respect to the occupation level ($0/++$) of these defects. In previous studies,^[11–16] the occupation of the M- or S-configurations was achieved either by illumination or by applying bias to the samples during cooling down.

The activation enthalpies of TDD0, TDD1, and TDD2 in configuration M are almost identical: 0.0726, 0.0692, and 0.0668 eV for the single-donor state and 0.1641, 0.1560, and 0.1469 eV for the double-donor states, respectively.^[8,9] However, in configuration S they were reported for the deep-donor state as ≈ 0.75 eV (TDD0),^[17] 0.48 eV (TDD1),^[18] and 0.29 eV (TDD2).^[18]

The electrical properties of the bistable TDDs (TDD0, TDD1, and TDD2) were investigated in previous studies.^[10,11,18,19] To date, the individual levels of TDD0, TDD1, and TDD2 were not resolved by electrical measurements. All reported DLTS peaks of TDDs were always broad and asymmetric.^[10,12,18,19] Previously, due to the limitations of the conventional DLTS technique, this effect could not be investigated properly. In the current study, we use Laplace DLTS to investigate this asymmetry. We are able to separate individual TDDs and identify TDD0, TDD1, and TDD2 by their bistability.


2. Experimental Section

For this study, we used the same sample material as studied by Bohne and Weber.^[19] The samples were cut from *n*-type CZ Si wafers with a phosphorous doping level of about 8.0×10^{14} – $1.0 \times 10^{15} \text{ cm}^{-3}$. The oxygen concentration in the samples was $[\text{O}_i] = 1 \times 10^{18} \text{ cm}^{-3}$, and the carbon concentration was $[\text{C}_s] = 1.6 \times 10^{16} \text{ cm}^{-3}$. The samples were chemically cleaned and pre-annealed at 770 °C for 30 min, and afterward, they were subjected to heat treatments at 460 °C for 20 or 60 min in argon atmosphere. After these thermal treatments, the samples were dipped in HF for a minute. Schottky diodes were produced by resistive evaporation of Au in vacuum onto the polished side

K. Gwozdz
Department of Quantum Technologies
Faculty of Fundamental Problems of Technology
Wrocław University of Science and Technology
Wybrzeże Wyspiańskiego 27, 50-370 Wrocław, Poland

Dr. V. Kolkovsky
Engineering Department
IPMS Fraunhofer
Dresden Maria-Reiche Str. 2, 01109 Dresden, Germany
E-mail: uladzimir.kalkouski@ipms.fraunhofer.de

Prof. J. Weber
Technische Universität Dresden
Institut für Angewandte Physik
01062 Dresden, Germany

 The ORCID identification number(s) for the author(s) of this article can be found under <https://doi.org/10.1002/pssa.201900302>.

DOI: 10.1002/pssa.201900302

of the samples at room temperature. Ohmic contacts were prepared by rubbing the back side of the samples with the eutectic InGa-alloy. The qualities of the Schottky and ohmic contacts were characterized by current–voltage (I – V) measurements. Capacitance–voltage (C – V) measurements were performed at 1 MHz with a Boonton 7200 capacitance meter. For the study of the bistable properties, we annealed the Schottky diodes under applied reverse bias annealing (RBA) of -4 or -8 V at 340 K for 60 min in the dark. Then, the diodes were cooled to 30 K under bias at a rate of ≈ 80 K min^{-1} . Zero bias annealing (ZBA) and cooling were performed by keeping the samples at 340 K for 30 min in the dark without reverse bias and identical cooling conditions. Laplace DLTS with two filling pulses was used to investigate the electronic properties (the activation enthalpy and the capture cross section) of deep levels and their concentrations.

3. Results and Discussion

We chose the sample doping and selected the annealing treatment to generate only TDD0, TDD1, and TDD2 with the Fermi level at 340 K between the occupancy levels of TDD1 and TDD2. Under these conditions, TDD2 behaves as a stable double-donor center, whereas TDD1 shows bistability and can be switched between the deep-donor state and the double-donor state. Bohne and Weber^[19] observed on the same sample material after annealing at 460 °C for 20 min only TDD1 and TDD2 by IR absorption measurements and found no traces of other TDDs. The double-donor TDD2 always appeared after cooling down the samples without illumination, whereas both double-donor states TDD1 and TDD2 were detected in the IR absorption spectrum after cooling down the samples under illumination. The authors detected the double-donor state of TDD1 and TDD2 in DLTS by annealing and cooling the samples under reverse bias and detected only the double-donor state of TDD2 after zero-bias annealing and cooling. Similar properties are expected in our samples.

Figure 1 shows two DLTS spectra of the Si sample annealed at 460 °C for 20 min. After annealing and cooling down the sample under ZBA, only a single DLTS peak is detected. Another DLTS peak with the maximum shifted in respect to that after ZBA is observed after annealing and cooling down the sample under RBA. The intensity of the DLTS peak after RBA is a factor of 1.4 larger in comparison with that after ZBA. Both DLTS peaks are relatively broad and asymmetric. We did not observe any other DLTS peak with a concentration greater than 10^{12} cm^{-3} in the sample.

To further investigate the electrical properties of these defects, the Laplace DLTS technique was used. Figure 2 shows Laplace DLTS spectra recorded in the same sample annealed at 460 °C for 20 min. The black curve shows the spectrum obtained in the sample after the cooling down without bias (ZBA). The blue curve is obtained from the same sample subjected to an additional annealing with a reverse bias of -8 V at 340 K for 20 min (RBA) and subsequent cooling down with the same reverse bias. One dominant peak labeled TDD2 is observed after ZBA with a concentration of $7.8 \times 10^{12} \text{ cm}^{-3}$. After RBA, two Laplace DLTS peaks labeled TDD2 and TDD1 are detected. The concentration of TDD2 is the same as after ZBA ($6.2 \times 10^{12} \text{ cm}^{-3}$), whereas that

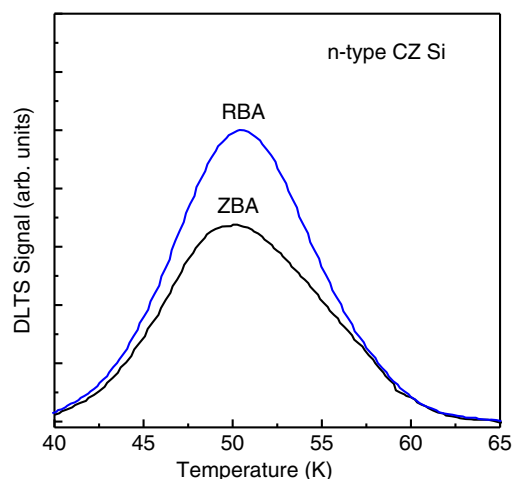


Figure 1. DLTS spectra recorded in n -type Si samples annealed at 460 °C for 20 min. The samples were subjected to annealing steps without (ZBA) and with a reverse bias of -8 V (RBA) at 340 K for 30 min.

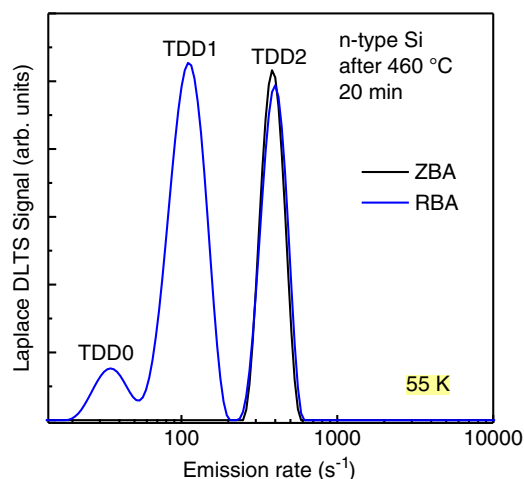


Figure 2. Laplace DLTS spectra recorded in the n -type Si sample annealed at 460 °C for 20 min. The sample was subjected to annealing steps at 340 K for 30 min and cooled down to measurement temperatures without (ZBA) and with a reverse bias of -8 V (RBA). The Laplace DLTS spectra were recorded with a reverse bias of -4 V and two filling pulses of -1 and -2 V.

of TDD1 is significantly higher (about $1.4 \times 10^{13} \text{ cm}^{-3}$). In addition to the dominant peaks TDD1 and TDD2, an additional satellite at lower emission rate is also observed in the RBA spectrum. Due to its bistability, we associate this peak with the TDD0 double-donor state. The concentration of the TDD0 peak is around $1.6 \times 10^{12} \text{ cm}^{-3}$.

Figure 3 presents Laplace DLTS spectra from a sample which was annealed at 460 °C for 60 min. Again, the black curve shows the sample after ZBA and the blue curve after RBA. After ZBA, two Laplace DLTS peaks labeled TDD2 and TDD1 are observed. The concentration of defects is $1.7 \times 10^{14} \text{ cm}^{-3}$ (TDD2) and $1 \times 10^{14} \text{ cm}^{-3}$ (TDD1). These concentrations are a factor of 20 higher compared with that of TDD2 after ZBA in Figure 2.

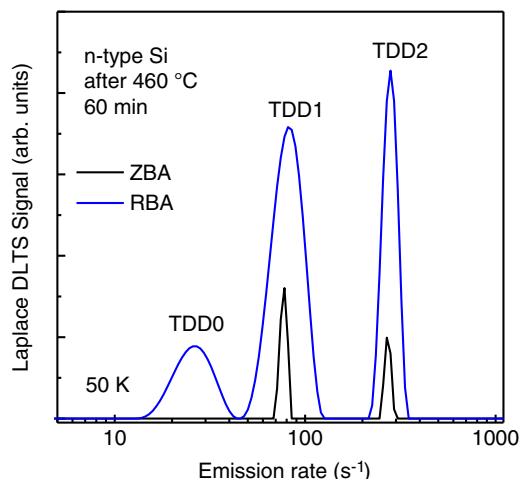


Figure 3. Laplace DLTS spectra recorded in the *n*-type Si sample annealed at 460 °C for 60 min. The sample was subjected to annealing steps at 340 K for 30 min and cooled down to measurement temperatures without (ZBA) and with a reverse bias of −8 V (RBA). The Laplace DLTS spectra were recorded with a reverse bias of −4 V and two filling pulses of −1 and −2 V.

After RBA, the additional Laplace DLTS peak TDD0 appears, whereas the intensity of TDD2 and TDD1 increases significantly in comparison with those observed after ZBA. The exact concentration of the peaks observed after RBA is impossible to be calculated: the defect concentration is comparable to the free carrier concentration in this sample and the measurement temperature is close to carrier freeze-out. However, from the *C*–*V* measurements, one can estimate that the sum of the TDDs observed in Figure 3 should be around $1.5 \times 10^{15} \text{ cm}^{-3}$.

The emission rates of the TDDs observed in Figure 2 and 3 are significantly enhanced by increasing the electric field in the depletion region of Si. However, we were not able to analyze this enhancement quantitatively due to the low temperature of the measurements, which is close to the carrier freeze-out temperature and due to the similar-field enhancement of the TDDs.

The Arrhenius plots of the TDDs observed in Figure 2 and 3 are shown in Figure 4. TDD0 could not be detected after RBA in the region with a low electric field. Therefore, the Arrhenius plots were recorded for a reverse bias of −4 V and two filling pulses of −1 and −2 V. The electrical parameters of the defects (their activation enthalpy and apparent capture cross section) are combined in Table 1.

In good agreement with Weber and Bohne,^[18,19] only a single Laplace DLTS peak TDD2 was observed after ZBA in the sample subjected to a heat treatment at 460 °C for 20 min. No traces of TDD0 and TDD1 were observed. The results are explained by the location of the Fermi level in-between the occupation levels (0/++) of TDD1 and TDD2 at the annealing temperature of 340 K. Indeed, the position of the Fermi level in the sample is around 0.25–0.27 eV at 340 K. The occupation levels of TDD1 and TDD2 are located at around 0.32 and 0.22 eV below the conduction band. Under these conditions, TDD1 and TDD2 are in the different configurations S and M, and as a result of the cooling without reverse bias, only TDD2 should appear in the Laplace DLTS spectrum. Similar conclusions were drawn from IR

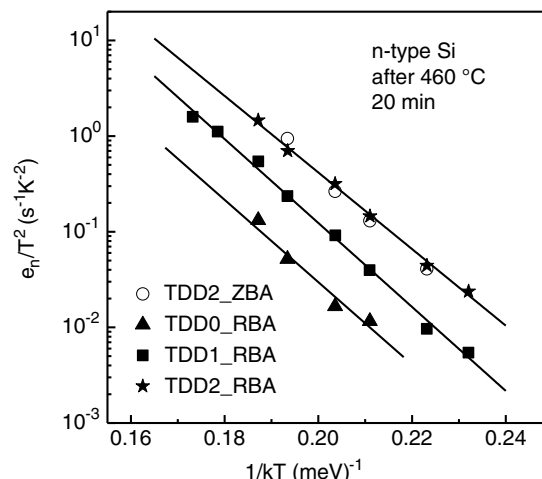


Figure 4. Arrhenius plots obtained for traps observed in Figure 2.

absorption measurements, where TDD2 was observed in the range of 430–530 cm^{-1} in similar samples after cooling down under illumination.^[18,19]

After RBA, two additional peaks TDD1 and TDD0 were observed, whereas the concentration of TDD2 remains almost constant. Under these conditions TDD0, TDD1, and TDD2 are all in the same M-configuration. Annealing at 340 K seems to be high enough to overcome the barrier needed for transformation from configuration S to configuration M. By cooling down the samples under reverse bias, the defects should be frozen-in in configuration M. The absence of TDD0 in the IR absorption spectra of Bohne and Weber^[19] can be related to the low concentration (around $1.6 \times 10^{12} \text{ cm}^{-3}$), which is below the detection limit for IR absorption.

In the sample annealed at 460 °C for 60 min, we attribute the dominant peaks to TDD1 and TDD2 after ZBA and RBA, respectively. The TDDs concentration in this sample is comparable with the doping concentration. The high carrier concentration results in a shift of the Fermi level above the occupation level of TDD2 at the annealing temperature. Under these conditions, ZBA annealing should freeze TDD0, TDD1, and TDD2 in the stable S configuration. No DLTS lines should be visible. In contrast, these peaks were observed in this sample already after ZBA. We explain this observation by the fact that during ZBA the thermal occupation of the TDD levels depends on the separation of the neutral deep-donor position of the S configuration from the donor levels of the M-configuration. For the sample with the lower TDD concentration, the occupation of

Table 1. The electrical parameters derived from the Arrhenius plots of the defects observed in Figure 2 and 3.

Defects	The activation enthalpy [meV]	The apparent capture cross section [cm^{-2}]
TDD0	103 ± 9	4×10^{-15}
TDD1	101 ± 4	1×10^{-14}
TDD2	94 ± 5	9×10^{-15}

the M configuration at 340 K under zero bias is too low to be detected by the DLTS technique.

Received: April 15, 2019
Revised: May 27, 2019
Published online: July 8, 2019

4. Conclusions

In the present study, we investigated the asymmetry of the DLTS peaks corresponding to TDDs observed in samples with a high oxygen concentration after heat treatments at 460 °C for 20 and 60 min. By using the Laplace DLTS technique, we successfully resolved three peaks and assigned them to the **double-donor levels of TDD0, TDD1, and TDD2**. We confirmed the bistability of these defects and investigated their electrical properties.

Acknowledgements

K.G. acknowledges the support from ERASMUS, a scholarship from the special-purpose grant awarded to the Faculty of Fundamental Problems of Technology at Wrocław University of Science and Technology by the Ministry of Science and Higher Education in 2018, for research and development of the young scientists and Ph.D. students, and the statutory Grant No. 0401/0009/17.

Conflict of Interest

The authors declare no conflict of interest.

Keywords

defects, Laplace deep-level transient spectroscopy, negative-U system, silicon, thermal double donors

- [1] C. S. Fuller, J. A. Ditzenberger, N. B. Hannay, E. Buehler, *Phys. Rev.* **1955**, 96, 833.
- [2] W. Kaiser, H. L. Frisch, H. Reiss, *Phys. Rev.* **1958**, 112, 1546.
- [3] W. Kaiser, *Phys. Rev.* **1957**, 105, 1751.
- [4] M. Tomassini, J. Veirman, R. Varache, E. Letty, S. Dubois, Ø. Nielsen, *J. Appl. Phys.* **2016**, 119, 084508.
- [5] Y. Hu, H. Schön, E. J. Øvrelid, Ø. Nielsen, L. Arnberg, *J. Appl. Phys.* **2012**, 111, 053101.
- [6] V. P. Markevich, M. Vaqueiro-Contreras, S. B. Lastovskii, L. I. Murin, M. P. Halsall, A. R. Peaker, *J. Appl. Phys.* **2018**, 124, 225703.
- [7] W. Götz, G. Pensl, W. Zulehner, *Phys. Rev. B* **1992**, 46, 4312.
- [8] L. I. Murin, V. P. Markevich, J. L. Lindstrom, M. Kleverman, *Physica B* **2003**, 340–342, 1046.
- [9] P. Wagner, J. Hage, *Appl. Phys. A* **1989**, 49, 123.
- [10] L. C. Kimmerling, J. L. Benton, *Appl. Phys. Lett.* **1981**, 39, 410.
- [11] Y. I. Latushko, L. F. Makarenko, V. P. Markevich, L. I. Murin, *Phys. Status Solidi A* **1986**, 93, K181.
- [12] A. Chantre, *Appl. Phys. Lett.* **1987**, 50, 1501.
- [13] V. D. Tkachev, L. F. Makarenko, V. P. Markevich, L. I. Murin, *Sov. Phys. Semicond.* **1984**, 18, 324.
- [14] L. F. Makarenko, V. P. Markevich, L. I. Murin, *Sov. Phys. Semicond.* **1985**, 19, 1192.
- [15] L. F. Makarenko, L. I. Murin, *Phys. Status Solidi B* **1988**, 145, 241.
- [16] L. F. Makarenko, *Phys. Status Solidi A* **1988**, 106, K153.
- [17] L. I. Murin, L. F. Makarenko, V. P. Markevich, in *Proc. 8th Int. School on Defects in Crystals*, Szczyrk, Poland, May, **1988**.
- [18] J. Weber, D. I. Bohne, *Early Stages of Oxygen Precipitation in Silicon*, NATO ASI Series 3, Vol. 17 (Ed: R. Jones), Kluwer Academic Publishers, Dordrecht **1996**, pp. 123–140.
- [19] D. I. Bohne, J. Weber, *Phys. Rev. B* **1993**, 47, 4037.